

## Diffractive Production at Collider Energies and Factorization

**Chung-I Tan**

Department of Physics, Brown University  
Providence, RI 02912

### Abstract

The most important consequence of Pomeron being a pole is the factorization property. However, due to Pomeron intercept being greater than 1, the extrapolated single diffraction dissociation cross section based on a classical triple-Pomeron formula is too large leading to a potential unitarity violation at Tevatron energies, which has been referred to as “Dino’s paradox”. We review our resolution which involves a proper implementation of final-state screening correction, with “flavoring” for Pomeron as the primary dynamical mechanism for setting the relevant energy scale. In this approach, factorization remains intact, and unambiguous predictions for double Pomeron exchange, doubly diffraction dissociation, etc., both at Tevatron and at LHC energies, can be made.

*To be published in a special issue of Physics Report  
in honor of Richard Slansky*

# 1 Introduction

One of the more interesting developments from recent collider experiments is the finding that hadronic total cross sections as well as elastic cross sections in the near-forward limit can be described by the exchange of a “soft Pomeron” pole, [1] *i.e.*, the absorptive part of the elastic amplitudes can be approximated by  $Im T_{a,b}(s, t) \simeq \beta_a(t) s^{\alpha_P(t)} \beta_b(t)$ . The Pomeron trajectory has two important features. [2] First, its zero-energy intercept is greater than one,  $\alpha_P(0) \equiv 1 + \epsilon$ ,  $\epsilon \simeq 0.08 \sim 0.12$ , leading to rising  $\sigma^{tot}(s)$ . Second, its Regge slope is approximately  $\alpha'_P \simeq 0.25 \sim 0.3 \text{ GeV}^{-2}$ , leading to the observed shrinkage effect for elastic peaks. The most important consequence of Pomeron being a pole is factorization. For a singly diffractive dissociation process, factorization leads to a “classical triple-Pomeron” formula, [4]

$$\frac{d\sigma}{dtd\xi} \rightarrow \frac{d\sigma^{classical}}{dtd\xi} \equiv F_{P/a}^{cl}(\xi, t) \sigma_{Pb}^{cl}(M^2, t), \quad (1)$$

where  $M^2$  is the missing mass variable and  $\xi \equiv M^2/s$ . The first term on the right-hand side of Eq. (1) is the so-called “Pomeron flux”, and the second term is the “Pomeron-particle” total cross section. Eq. (1) is in principle valid only when  $\xi^{-1}$  and  $M^2$  are both large, with  $t$  small and held fixed. However, with  $\epsilon \sim 0.1$ , it has been observed [5] that the extrapolated  $p\bar{p}$  single diffraction dissociation cross section,  $\sigma^{sd}$ , based on the standard triple-Pomeron formula is too large at Tevatron energies by as much as a factor of  $5 \sim 10$  and it could become larger than the total cross section.

Let us denote the singly diffractive cross section as a product of a “renormalization” factor and the classical formula,

$$\frac{d\sigma}{dtd\xi} = Z(\xi, t; s) \frac{d\sigma^{classical}}{dtd\xi}. \quad (2)$$

It was argued by K. Goulianos in Ref. [5] that agreement with data could be achieved by having an energy-dependent suppression factor,  $Z(\xi, t; s) \rightarrow Z_G(s) \equiv N(s)^{-1} \leq 1$ . [5][6][7] However, the modified triple-Pomeron formula no longer has a factorized form. An alternative suggestion has been made recently by P. Schlein. [8][9] It was argued that phenomenologically, after incorporating lower triple-Regge contributions, the renormalization factor for the triple-Pomeron contribution could be described by an  $\xi$ -dependent suppression factor,  $Z \rightarrow Z_S(\xi)$ .

In view of the factorization property for total and elastic cross sections, the “flux renormalization” procedure appears paradoxical and could undermine the theoretical foundation of a soft Pomeron as a Regge pole from a non-perturbative QCD perspective. We shall refer to this as “**Dino’s paradox**”. Finding a resolution that is consistent with Pomeron pole dominance for elastic and total cross sections at Tevatron energies will be the main focus of this study. In particular, we want to maintain the following factorization property,

$$\frac{d\sigma}{dtd\xi} \rightarrow \sum_k F_k(\xi, t) \sigma_k(M^2), \quad (3)$$

when  $\xi^{-1}$  and  $M^2$  become large.

A natural expectation for the resolution to this paradox lies in implementing a large screening correction to the classical triple-Pomeron formula. However, this appears too simplistic. In the absence of a new energy scale, a screening factor of the order  $5 \sim 10$ , if obtained, would apply both at Tevatron energies and at ISR energies. This indeed is the case for the eikonization analysis by Gotsman, Levin, and Maor, [11] as pointed out by Goulianos. Since a successful triple-Pomeron phenomenology exists up to ISR energies, a subtler explanation is required. We shall assume that any screening effect can supply at the most a  $10 \sim 20\%$  suppression and it cannot serve as the primary mechanism for explaining the paradox.

Triple-Regge phenomenology has had a long history. It has enjoyed many successes since early seventies, and it should emerge as a feature of any realistic representation of non-perturbative QCD for high energy scattering. In particular, it should be recognized that, up to ISR energies, triple-Pomeron phenomenology has provided a successful description for the phenomenon of diffractive dissociation. A distinguishing feature of the successful low-energy triple-Pomeron analyses is the value of the Pomeron intercept. It has traditionally been taken to be near 1, which would lead to total cross sections having constant “asymptotic values”. In contrast, the current paradox centers around the Pomeron having an intercept great than 1, e.g.,  $\epsilon \simeq 0.1$ .

Instead of trying to ask “how can one obtain a large suppression factor at Tevatron energies”, an alternative approach can be adopted. We could first determine the “triple-Pomeron” coupling by matching the diffractive cross section at the highest Tevatron energy. A naive extrapolation to lower energies via a standard triple-Pomeron formula would of course lead to too small a cross section at ISR energies. We next ask the question:

- Are there physics which might have been overlooked by others in mov-

ing down in energies?

- In particular, how can a high energy fit be smoothly interpolated with the successful low energy triple-Pomeron analysis using a Pomeron with intercept at 1, i.e.,  $\epsilon \simeq 0$ .

A key observation which will help in understanding our proposed resolution concerns the fact that, even at Tevatron energies, various “subenergies”, e.g., the missing mass squared,  $M^2$ , and the diffractive “gap”,  $\xi^{-1}$ , can remain relatively small, comparable to the situation of ISR energies for the total cross sections. (See Figure 1) Our analysis has identified the “**flavoring**” of Pomeron [12][13] as the primary dynamical mechanism for resolving the paradox. A proper implementation of final-state screening correction, (or **final-state unitarization**), assures a unitarized “gap distribution”. However, the onset of this suppression cannot take place at low energies; we find that flavoring sets this crucial energy scale. We also find that initial-state screening remains unimportant, consistent with the pole dominance picture for elastic and total cross section hypothesis at Tevatron energies.

In the usual usage of classical triple-Regge formulas, the basic energy scale is always in terms of  $s_0 \simeq 1 \text{ GeV}^2$ . We demonstrate that there are at least two other energy scales,  $s_r \equiv e^{y_r}$  and  $s_f \equiv e^{y_f}$ ,  $y_r \simeq 3 \sim 5$  and  $y_f \simeq 8 \sim 10$ , which must be incorporated properly. The first is associated with the physics of light quarks and the scale of chiral symmetry breaking. The second is the “flavoring” scale and is associated with “heavy flavor” production. In a non-perturbative QCD setting, both play an important role in our understanding of a bare Pomeron with an intercept greater than unity. [13]

In our treatment, initial-state screening remains unimportant, consistent with the pole dominance picture for elastic and total cross section hypothesis at Tevatron energies. The factor  $F_{a,\mathcal{P}}(\xi, t)$  from the Pomeron contribution will be referred to as a “unitarized Pomeron flux factor,” and we shall occasionally refer to our procedure as “**unitarization of Pomeron flux**”. We shall demonstrate that in our unitarization scheme the total renormalization factor has a factorized form,

$$Z(\xi, t; s) = Z_d(\xi, t) Z_m(M^2) = [S_f(\xi, t) R^2(\xi^{-1})] R(M^2), \quad (4)$$

where  $S_f$  is due to final-state screening, Eq. (32).  $R$  is a flavoring factor, given by Eq. (11), and there is one flavoring factor for each Pomeron propagator.

With the pole dominance hypothesis, we demonstrate that the unitarized flux factor must satisfy a normalization condition.

$$\int_{-\infty}^0 dt \int_0^1 d\xi F_{a,\mathcal{P}}(\xi, t) g_{\mathcal{PP}\mathcal{P}}(t) \xi^\epsilon \equiv \beta_a^{diff} < \beta_a(0), \quad (5)$$

where  $F_{a,\mathcal{P}}(\xi, t) \equiv Z_d(\xi, t) F_{a,\mathcal{P}}^{cl}(\xi, t)$ . The required damping to overcome the divergent behavior of  $F_{a,\mathcal{P}}^{cl}(\xi, 0)$  at small  $\xi$  comes from both the screening factor  $S_f(\xi, t)$  and the factor  $\xi^\epsilon$  from the “Pomeron-particle” total cross section.

In Sec. II, we first review the dynamics of soft Pomeron at low energies. We next discuss in Sec. III the origin of flavoring scale and indicate its relevance for diffractive dissociation cross sections. In Section IV, we explain why, given the Pomeron pole dominance hypothesis, the initial-state screening cannot be large at Tevatron energies and emphasize the importance of final-state absorption. We study in Sec. V the effect of final-state screening via an eikonal mechanism, consistent with the Pomeron pole dominance at collider energies.

Putting these together, we provide the final resolution to Dino’s paradox in Sec. VI. We present a phenomenological analysis which yields an estimate for the “high energy” triple-Pomeron coupling:

$$g_{\mathcal{PP}\mathcal{P}}(0) \simeq .14 \sim .20 \text{ mb}^{\frac{1}{2}}. \quad (6)$$

This value is consistent with our flavoring expectation, Eq. (34). Surprisingly, the amount of screening required at Tevatron energies seems to be very small. Predictions for other related cross sections are discussed in Sec. VII. Comparison of our approach to that of Refs. [5] and [8] as well as other comments are given in Sec. IIX.

## 2 Soft Pomeron at Low Energies

In order to be able to answer the questions we posed in the Introduction, it is necessary to first provide a dynamical picture for a soft Pomeron and to briefly review the notion of “Harari-Freund” duality.

### 2.1 Harari-Freund Duality

Although Regge phenomenology pre-dated QCD, it is important to recognize that it can be understood as a phenomenological realization of non-perturbative QCD in a “topological expansion”, e.g., the large- $N_c$  expansion.

In particular, an important feature of a large- $N_c$  expectation is emergence of the Harari-Freund two-component picture. [14]

For  $P_{lab} \leq 20$  GeV/c, it was recognized that the imaginary part of any hadronic two-body amplitude can be expressed approximately as the sum of two terms:

$$ImA(s, t) = R(s, t) + P(s, t).$$

From the s-channel point of view,  $R(s, t)$  represents the contribution of s-channel resonance while  $P(s, t)$  represents the non-resonance background. From the t-channel point of view,  $R(s, t)$  represents the contribution of “ordinary” t-channel Regge exchanges and  $P(s, t)$  represents the diffractive part of the amplitude given by the Pomeron exchange. Three immediate consequences of this picture are:

- (a) Imaginary parts of amplitudes which show no resonances should be dominated by Pomeron exchange, ( $R \simeq 0$ , and  $P \simeq \text{constant}$ ).
- (b) Imaginary parts of  $A(s, t)$  which have no Pomeron term should be dominated by s-channel resonances,
- (c) Imaginary parts of amplitudes which do not allow Pomeron exchange and show no resonances should vanish,

Point (b) can best be illustrated by partial-wave projections of  $\pi N \rightarrow \pi N$  scattering amplitudes from well-defined t-channel isospin exchanges. Point (c) is best illustrated by examining the  $K^+p \rightarrow K^0p$ , where, by optical theorem,  $ImA(K^+p \rightarrow K^0n) \propto \sigma_{tot}(K^+p) - \sigma_{tot}(K^0n)$ . The near-equality of these two cross sections, from the t-channel exchange view point, reflects the interesting feature of exchange degeneracy for secondary Reggeons. Finally, let us come to the point (a). From the behavior of  $\sigma_{\pi^\pm p}$ ,  $\sigma_{K^\pm p}$ ,  $\sigma_{pp}$  and  $\sigma_{\bar{p}p}$ , one finds that the near-constancy for the  $P$ -contribution corresponds to having an effective “low-energy” Pomeron intercept at 1, i.e.,

$$\alpha_P^{low}(0) \simeq 1.$$

## 2.2 Shadow Picture and Inelastic Production

A complementary treatment of Pomeron at low energies is through the analysis of inelastic production, which is responsible for the non-resonance background mentioned earlier. Diffraction scattering as the shadow of inelastic production has been a well established mechanism for the occurrence of a

forward peak. Analyses of data up to ISR energies have revealed that the essential feature of nondiffractive particle production can be understood in terms of a multiperipheral cluster-production mechanism. In such a picture, the forward amplitude at high energies is predominantly absorptive and is dominated by the exchange of a “bare Pomeron”.

In a “shadow” scattering picture, the “minimum biased” events are predominantly “short-range ordered” in rapidity and the production amplitudes can be described by a multiperipheral cluster model. Under a such an approximation to production amplitudes for the right-hand side of an elastic unitary equation,  $ImT(s, 0) = \sum_n |T_{2,n}|^2$ , one finds that the resulting elastic amplitude is dominated by the exchange of a Regge pole, which we shall provisionally refer to as the “bare Pomeron”. Next consider singly diffractive events. We assume that the “missing mass” component corresponds to no gap events, thus the distribution is again represented by a “bare Pomeron”. However, for the gap distribution, one would insert the “bare Pomeron” just generated into a production amplitude, thus leading to the classical triple-Pomeron formula.

Extension of this procedure leads to a “perturbative” expansion for the total cross section in the number of bare Pomeron exchanges along a multiperipheral chain. Such a framework was proposed long time ago, [15] with the understanding that the picture can make sense at moderate energies, provided that the intercept of the Pomeron is near one,  $\alpha(0) \simeq 1$ , or less.

However, with the acceptance of a Pomeron having an intercept greater than unity, this expansion must be embellished or modified. It is quite likely that the resolution for Dino’s paradox lies in understanding how such an effect can be accommodated within this framework, consistent with the Pomeron pole dominance hypothesis.

### 2.3 Bare Pomeron in Non-Perturbative QCD

In a non-perturbative QCD setting, the Pomeron intercept is directly related to the strength of the short-range order component of inelastic production and this can best be understood in a large- $N$  expansion. [16] In such a scheme, particle production mostly involves emitting “low-mass pions”, and the basic energy scale of interactions is that of ordinary vector mesons, of the order of 1 GeV. In a one-dimensional multiperipheral realization for the “planar component” of the large- $N$  QCD expansion, the high energy behavior of a  $n$ -particle total cross section is primarily controlled by its

longitudinal phase space,  $\sigma_n \simeq (g^4 N^2 / (n-2)!)(g^2 N \log s)^{n-2} s^{J_{eff}-1}$ . Since there are only Reggeons at the planar diagram level, one has  $J_{eff} = 2\alpha_R - 1$  and, after summing over  $n$ , one arrives at Regge behavior for the planar component of  $\sigma^{tot}$  where

$$\alpha_R = (2\alpha_R - 1) + g^2 N. \quad (7)$$

At next level of cylinder topology, the contribution to partial cross section increases due to its topological twists,  $\sigma_n \simeq (g^4 / (n-2)!) 2^{n-2} (g^2 N \log s)^{n-2} s^{J_{eff}-1}$ , and, upon summing over  $n$ , one arrives at a total cross section governed by a Pomeron exchange,  $\sigma_0^{tot}(Y) = g^4 e^{\alpha_P Y}$ , where the Pomeron intercept is

$$\alpha_P = (2\alpha_R - 1) + 2g^2 N. \quad (8)$$

Combining Eq. (7) and Eq. (8), we arrive at an amazing “bootstrap” result,  $\alpha_P \simeq 1$ .

Having a Pomeron intercept near 1 therefore depends crucially on the topological structure of large- $N$  non-Abelian gauge theories. [16] In this picture, one has  $\alpha_R \simeq .5 \sim .7$  and  $g^2 N \simeq .3 \sim .5$ . With  $\alpha' \simeq 1 \text{ GeV}^{-2}$ , one can also directly relate  $\alpha_R$  to the average mass of typical vector mesons. Since vector meson masses are controlled by constituent mass for light quarks, and since constituent quark mass is a consequence of chiral symmetry breaking, the Pomeron and the Reggeon intercepts are directly related to fundamental issues in non-perturbative QCD. This picture is in accord with the Harari-Freund picture for low-energy Regge phenomenology.

Finally we note that, in a Regge expansion, the relative importance of secondary trajectories to the Pomeron is controlled by the ratio  $e^{\alpha_R y} / e^{\alpha_P y} = e^{-(\alpha_P - \alpha_R) y}$ . It follows that there exists a natural scale in rapidity,  $y_r$ ,  $(\alpha_P - \alpha_R)^{-1} < y_r \simeq 3 \sim 5$ . The importance of this scale  $y_r$  is of course well known: When using a Regge expansion for total and two-body cross sections, secondary trajectory contributions become important and must be included whenever rapidity separations are below  $3 \sim 5$  units. This scale of course is also important for the triple-Regge region: There are two relevant rapidity regions: one associated with the “rapidity gap”,  $y \equiv \log \xi^{-1}$ , and the other for the missing mass,  $y_m \equiv \log M^2$ .

## 2.4 Conflict with Donnachie-Landshoff Picture

It has become increasingly popular to use the Donnachie-Landshoff picture [2] where Pomeron intercept above one, i.e.,  $\epsilon \sim 0.1$ . Indeed, it is



impressive that various cross sections can be fitted via Pomeron pole contribution over the entire currently available energy range. However, it should be pointed out that Donnachie-Landshoff picture is not consistent with the Harari-Freund picture at low energies. In particular, it under-estimates the Pomeron contribution at low energies, and it leads to a strong exchange degeneracy breaking.

It can be argued that the difference between these two approaches should not be important at high energies. This is certainly correct for total cross sections. However, we would like to stress that this is not the true for diffractive dissociation, even at Tevatron energies. This can best be understood in terms of rapidity variables,  $y$  and  $y_m$ . Since  $y + y_m \simeq Y$ ,  $Y \equiv \log s$ , it follows that, even at Tevatron energies, the rapidity range for either  $y$  or  $y_m$  is more like that for a total cross section at or below the ISR energies. (See Figure 1)

Therefore, details of diffractive dissociation cross section at Tevatron would depend on how a Pomeron is treated at relatively low subenergies.

### 3 Soft Pomeron and Flavoring

Consider for the moment the following scenario where one has two different fits to hadronic total cross sections:

- (a) “High energy fit”:  $\sigma_{ab}(y) \simeq \beta_a \beta_b e^{\epsilon y}$  for  $y \gg y_f$ ,
- (b) “Low energy fit”:  $\sigma_{ab}(y) \simeq \beta_a^{low} \beta_b^{low}$  for  $y \ll y_f$ .

That is, we envisage a situation where the “effective Pomeron intercept”,  $\epsilon_{eff}$ , increases from 0 to  $\epsilon \sim 0.1$  as one moves up in energies. In order to have a smooth interpolation between these two fits, one can obtain the following order of magnitude estimate  $\beta_p \simeq e^{-\frac{\epsilon y_f}{2}} \beta_p^{low}$ . Modern parameterization for Pomeron residues typically leads to values of the order  $(\beta_p)^2 \simeq 14 \sim 17$  mb. However, before the advent of the notion of a Pomeron with an intercept greater than 1, a typical parameterization would have a value  $(\beta_p^{low})^2 \simeq 35 \sim 40$  mb, accounting for a near constant Pomeron contribution at low energies. This leads to an estimate of  $y_f \sim 8$ , corresponding to  $\sqrt{s} \sim 50$  GeV. This is precisely the energy scale where a rising total cross section first becomes noticeable.

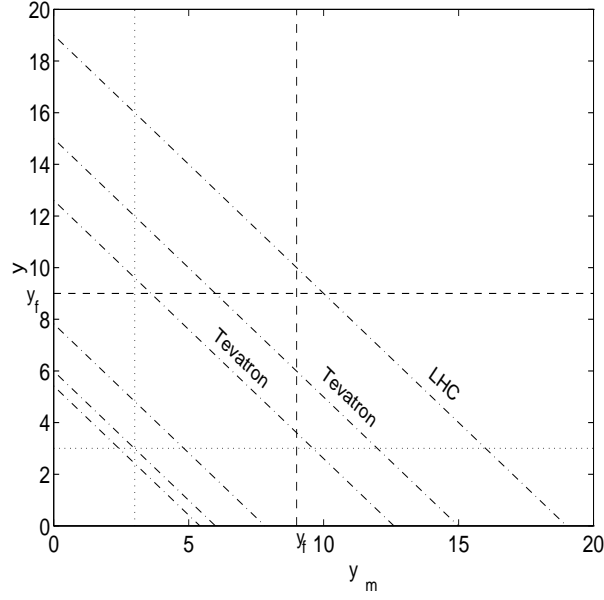


Figure 1: Phase space for single diffraction dissociation from ISR to LHC in terms of rapidity variables  $y \equiv \log \xi^{-1}$  and  $y_m \equiv \log M^2$ . The dashed lines are for “flavoring” scale,  $y_f$ , chosen to be 9 for illustration. Dotted lines are  $y_{min} \simeq 3$  lines for both  $y$  and  $y_m$ . The Dashed-dotted lines are constant center of mass energy lines for  $E_i$ ,  $i = 1, \dots, 6$ , equals to 15, 30, 60, 630, 1800, 14,000  $GeV$  respectively.

The scenario just described has been referred to as “flavoring”, the notion that the underlying effective degrees of freedom for Pomeron will increase as one moves to higher energies, [12] and it has provided a dynamical basis for understanding the value of Pomeron intercept in a non-perturbative QCD setting. [13] In this scheme, in order to extend a Regge phenomenology to low energies, both the Pomeron intercept and the Pomeron residues are **scale-dependent**. We shall review this mechanism shortly. However, we shall first introduce a scale-dependent formalism where the entire flavoring effect can be absorbed into a flavoring factor,  $R(y)$ , associated with each Pomeron propagator.

### 3.1 Effective intercept and Scale-Dependent Treatment

In order to be able to extend a Pomeron representation below the rapidity scale  $y \sim y_f$ , we propose the following **scale-dependent** scheme where we introduce a flavoring factor for each Pomeron propagator. Since each Pomeron exchange is always associated with energy variable  $s$ , (therefore a rapidity variable  $y \equiv \log s$ ), we shall parameterize the Pomeron trajectory function as

$$\alpha_{eff}(t; y) \simeq 1 + \epsilon_{eff}(y) + \alpha' t, \quad (9)$$

where  $\epsilon_{eff}(y)$  has the properties

- $\epsilon_{eff} \simeq \epsilon \simeq 0.1$  for  $y \gg y_f$ ,
- $\epsilon_{eff} \simeq \epsilon_o \equiv \alpha_{\mathcal{P}}^{low} - 1 \simeq 0$  for  $y < y_f$ .

For instance, exchanging such an effective Pomeron leads to a contribution to the elastic cross section  $T_{ab}(s, t) \propto s^{1+\epsilon_{eff}(y)+\alpha' t}$ . This representation can now be extended down to the region  $y \sim y_r$ . We shall adopt a particularly convenient parameterization for  $\epsilon_{eff}(y)$  in the next Section when we discuss phenomenological concerns.

To complete the story, we need also to account for the scale dependence of Pomeron residues. What we need is an “interpolating” formula between the high energy and low energy sets. Once a choice for  $\epsilon_{eff}(y)$  has been made, it is easy to verify that a natural choice is simply  $\beta_a^{eff}(y) = \beta_a e^{[\epsilon - \epsilon_{eff}(y)]y_f}$ . It follows that the total contribution from a “flavored” Pomeron corresponds to the following low-energy modification

$$T_{a,b}^{a,b}(y, t) \rightarrow R(y) T_{a,b}^{cl}(y, t), \quad (10)$$

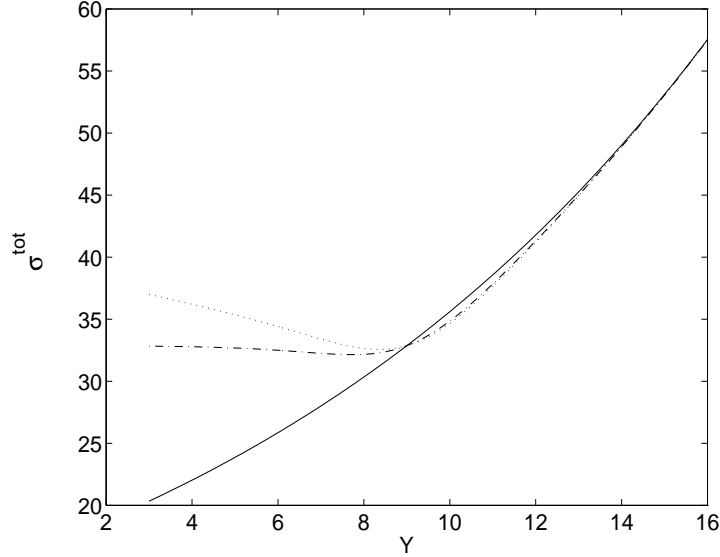


Figure 2: Effect of flavoring factor  $R(s)$  when applied to a standard rising cross section:  $\sigma^{cl} = \beta^2 s^\epsilon$ ,  $\epsilon = 0.1$  and  $\beta^2 = 16 \text{ mb}$ , given by the solid curve. With  $R(y)$  given by Eq. (31), the dashed-dotted curve has  $\epsilon_o = 0$ ,  $\lambda_f = 1$ , and flavoring scale  $y_f = 9$ , and the dotted curve corresponds to  $\epsilon_o = -0.04$ .

where  $T_{a,b}^{cl}(y, t) \equiv \beta_a \beta_b e^{(1+\epsilon+\alpha'_P t)y}$  is the amplitude according to a “high energy” description with a fixed Pomeron intercept, and

$$R(y) \equiv e^{-[\epsilon - \epsilon_{eff}(y)](y - y_f)}, \quad (11)$$

is a “flavoring” factor. The effect of this modification can best be illustrated via Figure 2.

This flavoring factor should be consistently applied as part of each “Pomeron propagator”. With the normalization  $R(\infty) = 1$ , we can therefore leave the residues alone, once they have been determined by a “high energy” analysis. For our single-particle gap cross section, since there are three Pomeron propagators, the renormalization factor is given by the following product:  $Z = R^2(y)R(y_m)$ . It is instructive to plot in Figure 3 this combination as a function of either  $\xi$  or  $M^2$  for various fixed values of total rapidity,  $Y$ .

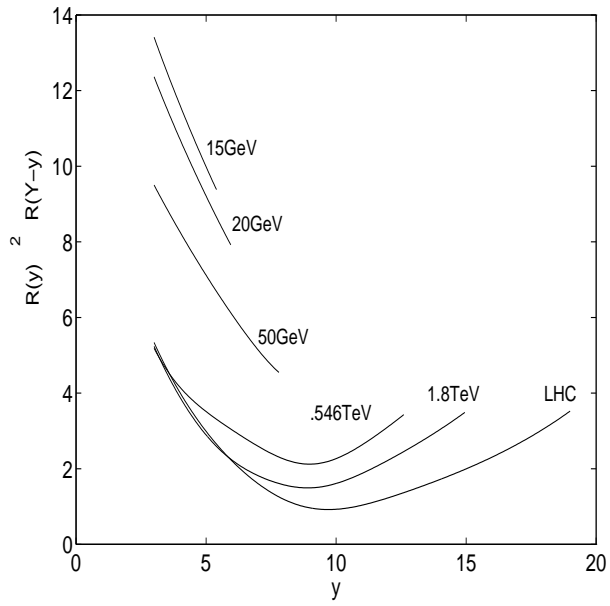


Figure 3: Renormalization factor due to flavoring alone,  $Z_f(\xi; s) \equiv R^2(\xi^{-1})R(M^2)$ , as a function of rapidity  $y = \log \xi^{-1}$  for various fixed center of mass energies. These curves correspond to parameters used for the solid line in Figure 4.

## 3.2 Flavoring of Bare Pomeron

We have proposed sometime ago that “baryon pair”, together with other “heavy flavor” production, provides an additional energy scale,  $s_f = e^{y_f}$ , for soft Pomeron dynamics, and this effect can be responsible for the perturbative increase of the Pomeron intercept to be greater than unity,  $\alpha_{\mathcal{P}}(0) \sim 1 + \epsilon$ ,  $\epsilon > 0$ . One must bear this additional energy scale in mind in working with a soft Pomeron. [13] That is, to fully justify using a Pomeron with an intercept  $\alpha_{\mathcal{P}}(0) > 1$ , one must restrict oneself to energies  $s > s_f$  where heavy flavor production is no longer suppressed. Conversely, to extrapolate Pomeron exchange to low energies below  $s_f$ , a lowered “effective trajectory” must be used. This feature of course is unimportant for total and elastic cross sections at Tevatron energies. However, it is important for diffractive production since both  $\xi^{-1}$  and  $M^2$  will sweep right through this energy scale at Tevatron energies.

Flavoring becomes important whenever there is a further inclusion of effective degrees of freedom than that associated with light quarks. This can again be illustrated by a simple one-dimensional multiperipheral model. In addition to what is already contained in the Lee-Veneziano model, suppose that new particles can also be produced in a multiperipheral chain. Concentrating on the cylinder level, the partial cross sections will be labeled by two indices,

$$\sigma_{p,q} \simeq (g^4/p!q!)2^{p+q}(g^2 N \log s)^p (g_f^2 N \log s)^q s^{J_{eff}-1}, \quad (12)$$

where  $q$  denotes the number of clusters of new particles produced. Upon summing over  $p$  and  $q$ , we obtain a “renormalized” Pomeron trajectory

$$\alpha_{\mathcal{P}}^{high} = \alpha_{\mathcal{P}}^{low} + \epsilon, \quad (13)$$

where  $\alpha_{\mathcal{P}}^{low} \simeq 1$  and  $\epsilon \simeq 2g_f^2 N$ . That is, in a non-perturbative QCD setting, the effective intercept of Pomeron is a dynamical quantity, reflecting the effective degrees of freedom involved in near-forward particle production.[13]

If the new degree of freedom involves particle production with high mass, the longitudinal phase space factor, instead of  $(\log s)^q$ , must be modified. Consider the situation of producing one  $N\bar{N}$  bound state together with pions, *i.e.*,  $p$  arbitrary and  $q = 1$  in Eq. (12). Instead of  $(\log s)^{p+1}$ , each factor should be replaced by  $(\log(s/m_{eff}^2))^{p+1}$ , where  $m_{eff}$  is an effective mass for the  $N\bar{N}$  cluster. In terms of rapidity, the longitudinal phase space factor becomes  $(Y - \delta)^{p+1}$ , where  $\delta$  can be thought of as a one-dimensional

“excluded volume” effect. For heavy particle production, there will be an energy range over which keeping up to  $q = 1$  remains a valid approximation. Upon summing over  $p$ , one finds that the additional contribution to the total cross section due to the production of one heavy-particle cluster is [12]  $\sigma_{q=1}^{tot} \sim \sigma_0^{total}(Y - \delta)(2g_f^2 N) \log(Y - \delta)\theta(Y - \delta)$ , where  $\alpha_P^{low} \simeq 1$ . Note the effective longitudinal phase space “threshold factor”,  $\theta(Y - \delta)$ , and, initially, this term represents a small perturbation to the total cross section obtained previously, (corresponding to  $q = 0$  in Eq. (12)),  $\sigma_0^{total}$ . Over a rapidity range,  $[\delta, \delta + \delta_f]$ , where  $\delta_f$  is the average rapidity required for producing another heavy-mass cluster, this is the only term needed for incorporating this new degree of freedom. As one moves to higher energies, “longitudinal phase space suppression” becomes less important and more and more heavy particle clusters will be produced. Upon summing over  $q$ , we would obtain a new total cross section, described by a renormalized Pomeron, with a new intercept given by Eq. (13).

We assume that, at Tevatron, the energy is high enough so that this kind of “threshold” effects is no longer important. How low an energy do we have to go before one encounter these effects? Let us try to answer this question by starting out from low energies. As we have stated earlier, for  $Y > 3 \sim 5$ , secondary trajectories become unimportant and using a Pomeron with  $\alpha \simeq 1$  becomes a useful approximation. However, as new flavor production becomes effective, the Pomeron trajectory will have to be renormalized. We can estimate for the relevant rapidity range when this becomes important as follows:  $y_f > 2\delta_0 + \langle q \rangle_{min} \delta_f$ . The first factor  $\delta_0$  is associated with leading particle effect, i.e., for proton, this is primarily due to pion exchange.  $\delta_f$  is the minimum gap associated with one heavy-mass cluster production, *e.g.*, nucleon-antinucleon pair production. We estimate  $\delta_0 \simeq 2$  and  $\delta_f \simeq 2 \sim 3$ , so that, with  $\langle q \rangle_{min} \simeq 2$ , we expect the relevant flavoring rapidity scale to be  $y_f \simeq 8 \sim 10$ .

## 4 Pomeron Dominance Hypothesis at Tevatron Energies

We shall first explore consequences of the observation that both total cross sections and elastic cross sections can be well described by a Pomeron pole exchange at Tevatron energies. Absorption correction, if required, seems to remain small. Since the singly diffractive cross section,  $\sigma^{sd}$ , is a sizable part of the total, it must also grow as  $s^\epsilon$ . This qualitative understanding can

be quantified in terms of a sum rule for “rapidity gap” cross sections. This in turn imposes a convergence condition on our unitarized Pomeron flux,  $F_{a,p}(\xi, t)$ .

To simplify the discussion, we shall first ignore transverse momentum distribution by treating the longitudinal phase space only. For instance, for singly diffraction dissociation, the longitudinal phase space can be specified by two rapidities,  $y \equiv \log(\xi^{-1})$  and  $y_m \equiv \log M^2$ . The first variable specifies the rapidity gap associated with the detected leading proton (or antiproton), and the second variable specifies the rapidity “span” of the missing mass distribution. At fixed  $s$ , they are constrained by  $y + y_m \simeq Y \equiv \log s$ , (see Figure 1), and we can speak of differential diffractive cross section  $d\sigma^{sd}/dy$ . We shall in what follows use  $\{\xi^{-1}, M^2\}$  and  $\{y \equiv \log \xi^{-1}, y_m \equiv \log M^2\}$  interchangeably. Dependence on transverse degrees of freedom can be re-introduced without much effort after completing the main discussion.

Consider the process  $a + b \rightarrow c + X^<$ , where the number of particles in  $X$  is unspecified. However, unlike the usual single-particle inclusive process, the superscript for  $X^<$  indicates that all particles in  $X$  must have rapidity less than that of the particle  $c$ , *i.e.*, the detected particle  $c$  is the one in the final state with the largest rapidity value. Kinematically, a single-gap cross section is identical to the singly diffraction dissociation cross section discussed earlier. Under the assumption where all transverse motions are unimportant, one has  $y_c \simeq y_a \equiv Y_{max}$  and the differential gap cross section,  $d\sigma^{gap}/dy$ , can also be considered as a function of  $y$  and  $y_m$ , with  $y + y_m \simeq Y$ .

Because the detected particle  $c$  has been singled out to be different from all other particles, this is no longer an inclusive cross section, and it does not satisfy the usual inclusive sum rules. Upon integrating over the rapidity gap  $y$  and summing over particle type  $c$ , no multiplicity enhancement factor is introduced and one obtains simply the total cross section, *i.e.*, a gap cross section satisfies the following exact sum rule,

$$\sum_c \int dy \frac{d\sigma_{ab \rightarrow c}^{gap}}{dy} \equiv \sum_c \sigma_{ab \rightarrow c}^{gap} = \sum_{n=2}^{\infty} \sigma_n = \sigma_{ab}^{tot}. \quad (14)$$

Interestingly, this allows an identification of the total cross section as a sum over specific gap cross sections,  $\sigma_{ab \rightarrow c}^{gap}$ , each is “derived” from a specific “leading particle” gap distribution. Since no restriction has been imposed on the nature of the “gap distribution”, *e.g.*, particle  $c$  can have different quantum numbers from  $a$ , the notion of a gap cross section is more general than a diffraction cross section.[17] It follows that the singly diffractive dissociation cross section,  $\sigma_{ab}^{sd}$ , is a part of  $\sigma_{ab \rightarrow a}^{gap}$ .



Consider next our factorized ansatz, Eq. (3). For  $y$  and  $y_m$  large, it leads to a gap distribution,  $d\sigma_{ab \rightarrow c}^{gap}/dy = e^{-y} F_{a \rightarrow c}(y) \sigma_b(y_m)$ . If  $\sigma_b(y_m) = g\beta_b e^{\epsilon y_m}$ , it follows that contribution from each gap distribution is Regge behaved,  $\sigma_{ab \rightarrow c}^{gap} \simeq \beta_a^c e^{\epsilon Y} \beta_b$ , where the total Pomeron residue is a sum of “partial residues”,

$$\beta_a = \sum_c \beta_a^c = \sum_c \int_0^\infty dy F_a^c(y) g e^{-(1+\epsilon)y}, \quad (15)$$

For above integral to converge, each flux factor must grow slower than  $e^{\epsilon y}$ . That is,  $F_a^c(y) e^{-\epsilon y} \rightarrow 0$  as  $y \rightarrow \infty$ . In a traditional Regge approach, the large rapidity gap behavior for each flux factor is controlled by an appropriate Regge propagator,  $e^{(\alpha_i + \alpha_j - 1)y}$ . Clearly a standard triple-Pomeron behavior with  $\alpha_P > 1$  is inconsistent with the pole dominance hypothesis. Unitarity correction must supply enough damping to provide convergence.

There is yet another way of expressing the consequence of the pole dominance hypothesis. Dividing each gap differential cross section by the total cross section, factorization of Pomeron leads to a “limiting distribution”:  $\rho_{ab}(y, Y) \rightarrow \rho_a(y) \equiv \sum_c \rho_a^c(y)$ . That is, the limit is independent of the total rapidity,  $Y$ , and the gap density is normalizable,  $\int_0^\infty dy \rho_a(y) = \sum_c \int_0^\infty dy \rho_a^c(y) = \sum_c (\beta_a^c / \beta_a) = 1$ . This normalization condition for the gap distribution is precisely Eq. (15).

Let us now restore the transverse distribution and concentrate on the diffractive dissociation contribution, which can be identified with the high  $M^2$  and high  $\xi^{-1}$  limit of  $d\sigma_{ab \rightarrow a}^{gap}(t, \xi; M^2)$ . In terms of  $\xi$ ,  $M^2$ , and  $t$ , the differential cross section at large  $M^2$  under our factorizable ansatz takes on the following form,  $d\sigma_{ab}^{sd}/dtd\xi \simeq F_{a,P}(\xi, t) \sigma_{P,b}^{cl}(M^2)$ , where  $\sigma_{P,b}^{cl}(M^2) = g_{PPPP}(t)(M^2)^\epsilon \beta_b(0)$ . It follows from Eq. (15) that  $F_{a,P}(\xi, t)$  must satisfy the following bound:

$$\int_{-\infty}^0 dt \int_{\xi_{min}(s)}^{\xi_{max}} d\xi F_{a,P}(\xi, t) g_{PPPP}(t) \xi^\epsilon \leq \int_{-\infty}^0 dt \int_0^1 d\xi F_{a,P}(\xi, t) g_{PPPP}(t) \xi^\epsilon \equiv \beta_a^{diff} < \beta_a(0). \quad (16)$$

The hypothesis of a Pomeron pole dominance for the total and elastic cross sections is of course only approximate. However, to the extent that absorptive corrections remain small at Tevatron energies, one finds that a modified Pomeron flux factor must differ from the “classical” Pomeron flux at small  $\xi$  in such a way so that the upper bound in Eq. (16) is satisfied. We shall refer to  $F_{a,P}(\xi, t)$  as the “unitarized Pomeron flux”. How this can be accomplished via final state screening will be discussed next. Note both the **similarity** and the **difference** between Eq. (16) and the “flux

normalization” condition mentioned in the Introduction. Here, this convergent integral yields asymptotically a finite number,  $\beta_a^{diff}$ , and the ratio  $\beta_a^{diff}/\beta_a(0)$  can be interpreted as the probability of having a diffractive gap at high energies.

## 5 Final-State Screening

The best known example for implementing the idea of “screening” in high energy hadronic collisions has been the “expanding disk” picture for rising total cross sections. Diffraction scattering as the shadow of inelastic production has been a well established mechanism for the occurrence of a forward peak. Analyses of data up to collider energies have revealed that the essential feature of nondiffractive particle production can be understood in terms of a multipartipheral cluster-production mechanism. In such a picture, the forward amplitude is predominantly absorptive and is dominated by the exchange of a “bare Pomeron”. If the Pomeron intercept is greater than one, it forces further unitarity corrections as one moves to higher energies. For instance, saturation of the Froissart bound can be next understood through an eikonal mechanism, with the absorptive eikonal  $\chi(s, b)$  given by the bare Pomeron amplitude in the impact-parameter space.

The main problem we are facing here is not so much on how to obtain a “most accurate” flux factor  $F_{a,\mathcal{P}}(\xi, t)$  at very small  $\xi$ . We are concerned with a more difficult conceptual problem of how to reconcile having a potentially large screening effect for diffraction dissociation processes and yet being able to maintain approximate pole dominance for elastic and total cross sections up to Tevatron energies. We shall show using an expanding disk picture that absorption works in such a way that inelastic scattering can only take place on the “edge” of disk. [18][19] Therefore, once applied using final-state screening, the effect of initial-state absorption will be small, hence allowing us to maintain Pomeron pole factorization for elastic and total cross sections.

### 5.1 Expanding Disk Picture

Let us briefly review this picture which also serves to establish notations. At high energies, a near-forward amplitude can be expressed in an impact-parameter representation via a two-dimensional Fourier transform,

$$T(s, t) \equiv 2is \int d^2\vec{b} e^{i\vec{q}\cdot\vec{b}} \tilde{f}(s, b), \quad \tilde{f}(s, b) = (4i\pi s)^{-1} \int d^2\vec{q} e^{-i\vec{b}\cdot\vec{q}} T(s, t), \quad (17)$$

where  $t \simeq -\vec{q}^2$ . Assume that the near-forward elastic amplitude at moderate energies can be described by a Born term, *e.g.*, that given by a single Pomeron exchange where we shall approximate it to be purely absorptive. Let us denote the contribution from the Pomeron exchange to  $\tilde{f}(s, b)$  as  $\chi(s, b)$ . With  $\alpha_{\mathcal{P}}(t) = 1 + \epsilon + \alpha'_{\mathcal{P}} t$ , and approximating  $\beta(t)$  by an exponential, we find  $\chi(s, b) \simeq X(s) e^{-(b^2/4B(s))}$ ,

$$X(s) \equiv \chi(s, 0) \simeq \frac{\sigma_0(s)}{4B(s)} \quad (18)$$

where  $B(s) = b_0 + \alpha'_{\mathcal{P}} \log s$  and  $\sigma_0(s) = \sigma_0 s^\epsilon$ . With  $\epsilon > 0$ , the Born approximation would eventually violate  $s$ -channel unitarity at small  $b$  as  $s$  increases. A systematic procedure which in principle should restore unitarity is the Reggeon calculus. However, our current understanding of dispersion-unitarity-relation is too qualitative to provide a definitive calculational scheme.

The key ingredient of “screening” correction is the recognition that the next order correction to the Born term must have a negative sign. (The sign of double-Pomeron cut contribution.) In an impact-representation, Reggeon calculus assures us that the correction can be represented as

$$\tilde{f}_1(s, b) \simeq -\frac{1}{2!} \mu(s) \chi(s, b)^2, \quad (19)$$

where  $\mu$  is positive. To go beyond this, one needs a model. A physically well-motivated model which should be meaningful at moderate energies and allows easy analytic treatment is the eikonal model. Writing  $\tilde{f}(s, b) = \tilde{f}_0(s, b) + \tilde{f}_1(s, b) + \tilde{f}_2(s, b) + \dots$ , the expansion alternates in sign, and with simple weights such that  $\tilde{f}(s, b) = [1 - e^{-\mu\chi(s, b)}]/\mu$ , and

$$T(s, t) = \left(\frac{2is}{\mu}\right) \int d^2\vec{b} e^{i\vec{q}\cdot\vec{b}} \{1 - e^{-\mu\chi(s, b)}\}. \quad (20)$$

Conventional eikonal model has  $\mu = 1$ . We keep  $\mu \leq 1$  here so as to allow the possibility that screening is “imperfect”.

Observe that the eikonal derived from the Pomeron exchange,  $\chi(s, b)$ , is a monotonically decreasing function of  $b^2$ , taking on its maximum value  $X(s)$  at  $b^2 = 0$ , which increases with  $s$  due to  $\epsilon > 0$ . The eikonal drops to zero at large  $b^2$  and is of the order 1 at a radius,  $b_c(s) \simeq \sqrt{B(s) \log \mu X(s)} \sim \log s$ . Within this radius,  $\tilde{f}(s, b) = O(1)$  and it vanishes beyond. This is the “expansion disk” picture of high energy scattering, leading to an asymptotic total cross section  $O(b_c(s)^2)$ .

## 5.2 Inelastic Screening

In order to discuss inelastic final-state screening, we follow the “shadow” scattering picture in which the “minimum biased” events are predominantly “short-range ordered” in rapidity and the production amplitudes can be described by a multiperipheral cluster model. Substituting these into the right-hand side of an elastic unitary equation,  $ImT(s, 0) = \sum_n |T_{2,n}|^2$ , one finds that the resulting elastic amplitude is dominated by the exchange of a Regge pole, which we shall provisionally refer to as the “bare Pomeron”. Next consider singly diffractive events. We assume that the “missing mass” component corresponds to no gap events, thus the distribution is again represented by a “bare Pomeron”. However, for the gap distribution, one would insert the “bare Pomeron” just generated into a production amplitude, thus leading to the classical triple-Pomeron formula.

Extension of this scheme leads to a “perturbative” treatment for the total cross section in the number of bare Pomeron exchanges along a multiperipheral chain. Such a scheme was proposed long time ago, [15] with the understanding that the picture could make sense at moderate energies, provided that the intercept of the Pomeron is one,  $\alpha(0) \simeq 1$ , or less. However, with the acceptance of a Pomeron having an intercept greater than unity, this expansion must be embellished. Although it is still meaningful to have a gap expansion, one must improve the descriptions for parts of a production amplitude involving large rapidity gaps by taking into account absorptions for the gap distribution. We propose that this “partial unitarization” be done for each gap separately, thus maintaining the factorization property along each short-range ordered sector. This involves final-state screening, and, for singly diffraction dissociation, it corresponds to the inclusion of “enhanced Pomeron diagrams” in the triple-Regge region.

To simplify the notation, we shall use the energy variable,  $\xi^{-1}$ , and the rapidity gap variable,  $y = \log(\xi^{-1})$ , interchangeably. Let’s express the total unitarized contribution to a gap cross section in terms of a “unitarized flux” factor,  $F(y, t) \equiv (e^y/16\pi)|g_d(y, t)|^2 \equiv (1/16\pi\xi)|f_d(\xi, t)|^2$ , so that it reduces to the classical triple-Pomeron formula as its Born term. That is, the corresponding Born amplitude for  $f_d(\xi, t)$  is the “square-root” of the triple-Pomeron contribution to the classical formula,  $f_P^d(\xi, t) = \beta_P(t)(\xi^{-1})^{(\alpha_P(t)-1)}$ . Screening becomes important if large gap becomes favored, *i.e.*, when  $\epsilon > 0$ .

Let us work in an impact representation,  $g(y_d, t) \equiv 2i \int d^2\vec{q} e^{i\vec{b}\cdot\vec{q}} \tilde{g}_d(y_d, b)$ . Consider an expansion  $\tilde{g}(y, b) = \chi_d(y, b) + \tilde{g}_1(y, b) + \tilde{g}_2(y, b) + \dots$  where, under the usual exponential approximation for the  $t$ -dependence, the Fourier

transform for the Born term is  $\chi_d(y, b) = \frac{\sigma^d(y)}{4B_d(y)} e^{-\frac{b^2}{4B_d(y)}}$ , with  $B_d(y) = b_d + \alpha'_{\mathcal{P}} y$  and  $\sigma^d(y) = \sigma_d e^{\epsilon y}$ . The key physics of absorption is

$$\tilde{g}_1(y, b) \simeq -\mu_d \chi(y, b) \chi_d(y, b). \quad (21)$$

The proportionality constant  $\mu_d$  can be different from the constant  $\mu$  introduced earlier for the elastic screening, either for kinematic or dynamic reasons, or both. For a generalized eikonal approximation, one has  $\tilde{g}(y, b) = \chi_d \{1 - \mu_d \chi + \frac{1}{2!} (\mu_d \chi)^2 - \dots\} = \chi_d(y, b) e^{-\mu_d \chi(y, b)}$ . If we define the “final-state screening” factor as the ratio between the unitarized flux factor and the classical triple-Pomeron formula,  $F_{a,\mathcal{P}}(y, t) = S_f^{(0)}(y, t; X) F_{a,\mathcal{P}}^{\text{cl}}(y, t)$ , we then have

$$S_f^{(0)}(y, t; X) = |f_d(y, t)/f_d^{\text{cl}}(y, t)|^2. \quad (22)$$

We shall use this expression as a model for probing the physics of inelastic screening in an expanding disk picture.

Let us examine this eikonal screening factor in the forward limit,  $t = 0$ , where

$$S_f^{(0)}(y, 0; X)^{\frac{1}{2}} = \frac{\int db^2 \chi_d(y, b) e^{-\mu_d \chi(y, b)}}{\int db^2 \chi_d(y, b)}. \quad (23)$$

Unlike the elastic situation, the integrand of the numerator is strongly suppressed both in the region of large  $b^2$  and in the region “inside” the expanding disk. **The only significant contribution comes from a “ring” region near the edge of the expanding disk.** [18][20] Since the value of the integrand is of  $O(1)$  there, one finds that the numerator varies with energy only weakly. On the other hand, the denominator is simply  $\sigma^d(y)$ , which increases as  $e^{\epsilon y}$ . Therefore, this leads to an exponential cutoff in  $y$ ,  $S_f^{(0)}(y, 0; X) \sim e^{-2\epsilon y}$ . This damping factor precisely cancels the  $\xi^{-2\epsilon}$  behavior from the classical triple-Pomeron formula at small  $\xi$ , leading to a unitarized Pomeron flux factor.

To be more precise, let us work in a simpler representation for  $S_f^{(0)}(y, 0; X)$  by changing the variable  $b^2 \rightarrow z \equiv e^{-b^2/4B(y)}$ . With our gaussian approximation, one finds that

$$S_f^{(0)}(y, 0; X) = \{r \int_0^1 dz z^{r-1} e^{-xz}\}^2|_{x=\mu_d X(y), r=r(y)}, \quad (24)$$

where  $r(y) \equiv B(y)/B_d(y)$ . This expression can be expressed as  $\{rx^{-r}\Gamma(x, r)\}^2|_{x=\mu_d X(y), r=r(y)}$ , where  $\Gamma(x, r) = \int_0^x dz z^{r-1} e^{-z}$  is the incomplete Gamma function. In this

representation, one easily verifies that the screening factor has the desired properties: As  $\mu_d \rightarrow 0$ , screening is minimal and one has  $S_f^{(0)}(y, 0; X) \rightarrow 1$ . On the other hand, for  $y$  large,  $X(y)$  increases so that  $S_f^{(0)}(y, 0; X) \rightarrow [\mu_d X(y)]^{-2}$ , as anticipated.

Similarly, we find that the logarithmic width for the unitarized flux  $D(y, t)$  at  $t = 0$  has increased from  $2B_d$  to  $2B_d^{eikonal}$  where  $B_d^{eikonal} = B_d \{-r \frac{d}{dr} \log \int_0^1 dz z^{r-1} e^{-xz}\}_{x=\mu_d X(y), r=r(y)}$ . As  $\mu_d \rightarrow 0$ ,  $B_d^{eikonal} \rightarrow B_d$ . For  $y$  very large,  $B_d^{eikonal} \rightarrow B \log \mu_d X(y) \sim b_c(y)^2 \propto y^2$ . This corresponds to a faster shrinkage than that of ordinary Regge behavior. Averaging over  $t$ , one finds at large diffractive rapidity  $y$ , the final-state screening provides an average damping

$$\langle S_f \rangle \rightarrow e^{-2\epsilon y} = \xi^{2\epsilon}. \quad (25)$$

This leads to a unitarized Pomeron flux,  $F_{a,p}(\xi, t)$ , which automatically satisfies the upper bound, Eq. (16), derived from the Pomeron pole dominance hypothesis.[20]

## 6 Final Recipe

Having explained earlier the notion of flavoring and its effects both on Pomeron intercept and on its residues, we must build in this feature for the final-state screening. As we have shown in the last section, inelastic screening is primarily driven by the “unitarity saturation” of the elastic eikonal, Eq. (18). However, because of flavoring, screening sets in only when the Pomeron flavoring scale is reached. This picture is consistent with the fact that, while low-mass diffraction seems to be highly suppressed, high-mass diffraction remains strong at Tevatron energies.

Since a Pomeron exchange enters as a Born term, i.e., the eikonal for either the elastic or the inelastic diffractive production, flavoring can easily be incorporated if we multiply both  $\chi(y, b)$  and  $\chi_d(y, b)$  by a flavoring factor  $R(y)$ . That is, if we adopt a generalized eikonal model for final-state screening, the desired screening factor becomes

$$S_f(\xi, t) = S_f^{(0)}(y, t; R(y)X(y), \mu_d) \quad (26)$$

where  $S_f^{(0)}$  is given by Eq. (22). We have also explicitly exhibited the dependence on the maximal value of the flavored elastic eikonal,  $RX$ , and on the effectiveness parameter  $\mu_d$ .

Let's now put all the necessary ingredients together and spell out the details for our proposed resolution to Dino's paradox. Our **final recipe** for the Pomeron contribution to single diffraction dissociation cross section is

$$\frac{d\sigma}{dt d\xi} = F_{a,\mathcal{P}}(\xi, t) \sigma_{\mathcal{P}b}(M^2), \quad (27)$$

where the unitarized flux,  $F_{a,\mathcal{P}}$ , and the Pomeron-particle cross section,  $\sigma_{\mathcal{P}b}$ , are given in terms of their respective classical expressions by  $F_{a,\mathcal{P}}(\xi, t) \equiv Z_d(\xi, t) F_{a,\mathcal{P}}^{cl}(\xi, t)$  and  $\sigma_{\mathcal{P}b}(M^2) \equiv Z_m(M^2) \sigma_{\mathcal{P}b}^{cl}(M^2, t)$ . It follows that the total suppression factor is

$$Z(\xi, t; M^2) = Z_d(\xi, t) Z_m(M^2) = [S_f(\xi, t) R^2(\xi^{-1})] R(M^2), \quad (28)$$

with the screening factor given by Eq. (26) and the flavoring factor given by Eq. (11). Finally, we point out that the integral constraint for the unitarized flux, Eq. (5), when written in terms of these suppression factors, becomes

$$\int_{-\infty}^0 dt \int_0^1 d\xi S_f(\xi, t) R^2(\xi^{-1}) F_{a,\mathcal{P}}^{cl}(\xi, t) g(t) \xi^\epsilon = \beta_a^{diff} < \beta_a(0), \quad (29)$$

where  $F_{a,\mathcal{P}}^{cl}(\xi, t) \equiv (1/16\pi) \beta_a(t)^2 (\xi^{-1})^{2\alpha_{\mathcal{P}}(t)-1}$ .

## 6.1 Phenomenological Parameterizations

Both the screening function and the flavoring function depend on the effective Pomeron intercept, and we shall adopt the following simple parameterization. The transition from  $\alpha^{old}(0) = 1 + \epsilon_o$  to  $\alpha^{new}(0) = 1 + \epsilon$  will occur over a rapidity range,  $(y_f^{(1)}, y_f^{(2)})$ . Let  $y_f \equiv \frac{1}{2}(y_f^{(1)} + y_f^{(2)})$  and  $\lambda_f^{-1} \equiv \frac{1}{2}(y_f^{(2)} - y_f^{(1)})$ . Similarly, we also define  $\bar{\epsilon} \equiv \frac{1}{2}(\epsilon + \epsilon_o)$  and  $\Delta \equiv \frac{1}{2}(\epsilon - \epsilon_o)$ . A convenient parameterization for  $\epsilon_{eff}$  we shall adopt is

$$\epsilon_{eff}(y) = [\bar{\epsilon} + \Delta \tanh \lambda_f(y - \bar{y}_f)]. \quad (30)$$

The combination  $[\epsilon - \epsilon_{eff}(y)]$  can be written as  $(2\bar{\epsilon}) [1 + (s/s_f)^{2\lambda_f}]^{-1}$  where  $s_f = e^{y_f}$ . Combining this with Eq. (11), we arrive at a simple parameterization for our flavoring function

$$R(s) \equiv \left(\frac{s_f}{s}\right)^{(2\bar{\epsilon}) [1 + (\frac{s}{s_f})^{2\lambda_f}]^{-1}}. \quad (31)$$

With  $\alpha_{\mathcal{P}}^{old} \simeq 1$ , we have  $\epsilon_o \simeq 0$ ,  $\bar{\epsilon} \simeq \Delta \simeq \epsilon/2$ , and we expect that  $\lambda_f \simeq 1 \sim 2$  and  $y_f \simeq 8 \sim 10$  are reasonable range for these parameters. [21]

To complete the specification, we need to provide a more phenomenological description for the final-state screening factor. First, we shall approximate the screening factor by an exponential in  $t$ :

$$S_f(y, t) \simeq S_f(y, 0)e^{\Delta B_d(y)t}. \quad (32)$$

where  $S_f(y, 0) = \{r x^{-r} \Gamma(x, r)\}^2$ , with  $x = \mu_d R(y) X(y)$  and  $r = r(y)$ . The width,  $\Delta B_d(y)$ , can be obtained by a corresponding substitution. Note that  $S_f(y, 0)$  depends on  $B(y)$ ,  $B_d(y)$ ,  $X(y)$ , and  $\mu_d$ . Phenomenological studies allow us to approximate  $B(y) \simeq b_0 + .25y$  and  $B_d(y) \simeq b_d + .25y$ ,  $b_d \simeq b_0/2 \sim 2.3 \text{ GeV}^{-2}$ .

The only quantity left to be specified is the effectiveness parameter  $\mu_d$ . Since the physics of final-state screening is that driven by a Pomeron with intercept greater than unity, the relevant rapidity scale is again  $y_f$ . Let us fix  $\mu_d$  first by requiring that screening is small for  $y < y_f$ , *i.e.*,  $S_f(y, 0) \sim 1$  as one moves down in rapidity from  $y_f$  to  $y_r$ . Similarly, we expect screening to approach its full strength as one moves past the flavoring threshold  $y_f$ . We thus find it economical to parameterize

$$\mu_d(y) \simeq (\mu_0/2)\{1 + \tanh[\lambda_d(y - \bar{y}_f)]\}, \quad (33)$$

and we expect  $\bar{y}_f \sim y_f$  and  $\lambda_d \sim \lambda_f$ . This completes the specification of our unitarization procedure.

## 6.2 High Energy Diffractive Dissociation

The most important new parameter we have introduced for understanding high energy diffractive production is the flavoring scale,  $s_f = e^{y_f}$ . We have motivated by way of a simple model to show that a reasonable range for this scale is  $y_f \simeq 8 \sim 10$ . Quite independent of our estimate, it is possible to treat our proposed resolution phenomenologically and determine this flavoring scale from experimental data.

It should be clear that one is not attempting to carry out a full-blown phenomenological analysis here. To do that, one must properly incorporate other triple-Regge contributions, *e.g.*, the  $\mathcal{PPR}$ -term for the low- $y_m$  region, the  $\pi\pi\mathcal{P}$ -term and/or the  $\mathcal{RRP}$ -term for the low- $y$  region, etc., particularly for  $\sqrt{s} \leq \sqrt{s_f} \sim 100 \text{ GeV}$ . What we hope to achieve is to provide a “caricature” of the interesting physics involved in diffractive production at collider energies through our introduction of the screening and the flavoring factors. [21]



Let us begin by first examining what we should expect. Concentrate on the triple-Pomeron vertex  $g(0)$  measured at high energies. Let us for the moment assume that it has also been measured reliably at low energies, and let us denote it as  $g^{low}(0)$ . Our flavoring analysis indicates that these two couplings are related by

$$g(0) \simeq e^{-(\frac{3\epsilon y_f}{2})} g^{low}(0). \quad (34)$$

With  $\epsilon \simeq 0.08 \sim 0.1$  and  $y_f \simeq 8 \sim 10$ , using the value  $g^{low}(0) = 0.364 \pm 0.025 \text{ mb}^{\frac{1}{2}}$ , [22] we expect a value of  $0.12 \sim 0.18 \text{ mb}^{\frac{1}{2}}$ . Denoting the overall multiplicative constant for our renormalized triple-Pomeron formula by  $K$ ,

$$K \equiv \frac{\beta_a^2(0) g_{PPP}(0) \beta_b(0)}{16\pi}. \quad (35)$$

With  $\beta_p^2 \simeq 16 \text{ mb}$ , we therefore expect  $K$  to lie between the range  $.15 \sim .25 \text{ mb}^2$ .

We begin testing our renormalized triple-Pomeron formula by first turning off the final-state screening, *i.e.*, setting  $S_f = 1$ . We determine the overall multiplicative constant  $K$  by normalizing the integrated  $\sigma^{sd}$  to the measured CDF  $\sqrt{s} = 1800 \text{ GeV}$  value.[23] With  $\epsilon = 0.1$ ,  $\lambda_f = 1$ , this is done for a series of values for  $y_f = 7, 8, 9, 10$ . We obtain respective values for  $K = .24, 0.21, 0.18, 0.15$ , consistent with our flavoring expectation. As a further check on the sensibility of these values for the flavoring scales, we find for the ratio  $\rho \equiv \sigma^{sd}(546)/\sigma^{sd}(1800)$  the values 0.63, 0.65, 0.68, 0.72 respectively. This should be compared with the CDF result of 0.834.

Next we consider screening. Note that screening would increase our values for  $K$ , which would lead to large values for  $g$ . Since we have already obtained values for triple-Pomeron coupling which are of the correct order of magnitude, the only conclusion we can draw is that, at Tevatron, screening cannot be too large. With our parameterization, we find that screening is rather small at Tevatron energies, with  $\mu_0 \simeq 0.0 \sim 0.2$ . This comes as somewhat a surprise! Clearly, screening will become important eventually at higher energies. After flavoring, the amount of screening required at Tevatron is apparently greatly reduced.

Having shown that our renormalized triple-Pomeron formula does lead to sensible predictions for  $\sigma^{sd}$  at Tevatron, we can improve the fit by enhancing the  $PPR$ -term as well as  $RRP$ -terms which can become important. Instead of introducing a more involved phenomenological analysis, we simulate the

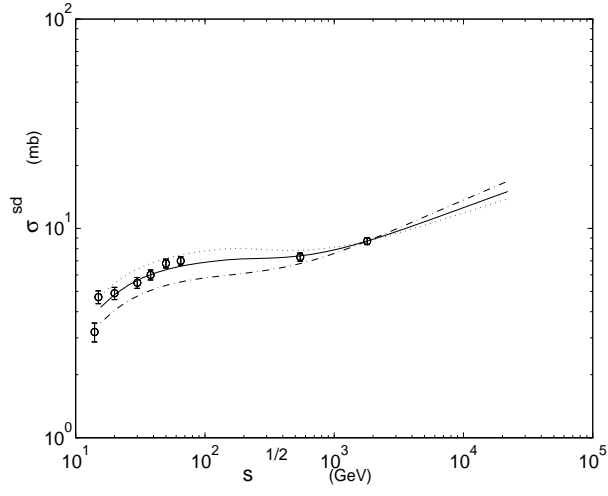


Figure 4: Fits to representative single diffraction dissociation cross sections from ISR to Tevatron.[5] The solid line corresponds to  $\epsilon = 0.08$ ,  $\epsilon_o = -0.07$ ,  $\lambda_f = 1$ ,  $y_f = 9$ , with a small amount of final-state screening,  $\mu_0 = 0.1$ . The dotted and the dashed-dotted curves correspond to  $\mu_0 = 0.2$  and  $\mu_0 = 0$ , i.e., no screening, respectively.

desired low energy effect by having  $\epsilon_o \simeq -0.06 \sim -0.08$ . A remarkably good fit results with  $\epsilon = 0.08 \sim 0.09$ ,  $y_f = 9$  and  $\mu_0 \simeq 0 \sim 0.2$ . [21] This is shown in Figure 4. The ratio  $\rho$  ranges from  $0.78 \sim 0.90$ , which is quite reasonable. The prediction for  $\sigma^{sd}$  at LHC is  $12.6 \sim 14.8 \text{ md}$ .

Our fit leads to a triple-Pomeron coupling in the range of

$$g_{\mathcal{P}\mathcal{P}\mathcal{P}}(0) \simeq .12 \sim .18 \text{ mb}^{\frac{1}{2}}, \quad (36)$$

exactly as expected. Interestingly, the triple-Pomeron coupling quoted in Ref. [5] ( $g(0) = 0.69 \text{ mb}^{\frac{1}{2}}$ ) is actually a factor of 2 larger than the corresponding low energy value. [22] Note that this difference of a factor of 5 correlates almost precisely with the flux renormalization factor  $N(s) \simeq 5$  at Tevatron energies.

We believe, with care, the physics of flavoring and final-state screening can be tested independent of the specific parameterizations we have proposed here. In particular, because our unitarized Pomeron flux approach retains factorization along the “missing mass” link, unambiguous predictions can be made for other processes involving rapidity gaps.

## 7 Predictions for Other Gap Cross Sections

For both double Pomeron exchange (DPE) and doubly diffractive (DD) processes, one is dealing with three rapidity variables which can become large. We will treat these two cases first before turning to more general situations.

### 7.1 Prediction for DPE Cross Sections:

For double Pomeron exchange (DPE), we are dealing with events with two large rapidity gaps. The final state configuration can be specified by five variables,  $t_1$ ,  $t_2$ ,  $\xi_1$ ,  $\xi_2$ , and  $M^2$ . For  $t_1$  and  $t_2$  small, one again has a constraint,  $\xi_1^{-1} M^2 \xi_2^{-1} \simeq s$ . Alternatively, we can work with rapidity variables,  $y_1 \equiv \log(\xi_1^{-1})$ ,  $y_2 \equiv \log(\xi_2^{-1})$ , and  $y_m \equiv \log M^2$ , with  $y_1 + y_m + y_2 \simeq Y = \log s$ . The appropriate DPE differential cross section can be written down, with no new free parameter. Let us introduce a renormalization factor

$$\frac{d\sigma}{dy_1 dt_1 dy_2 dt_2} = Z_{DPE}(y_1, t_1, y_m, y_2, t_2) \frac{d\sigma^{classical}}{dy_1 dt_1 dy_2 dt_2}. \quad (37)$$

One immediately finds that, using Pomeron factorization for the missing mass variable,

$$Z_{DPE} = [S_f(y_1, t_1)R(y_1)^2]R(y_m)[S_f(y_2, t_2)R(y_2)^2] = Z_d(\xi_1, t_1)Z_m(M^2)Z_d(\xi_2, t_2). \quad (38)$$

Alternatively, we can express this cross section in terms of singly diffractive dissociation cross sections as

$$\frac{d\sigma_{ab}}{dy_1 dt_1 dy_2 dt_2} = \left\{ \frac{d\sigma_{ab}}{dy_1 dt_1} \right\} \{ R(y_m) \sigma_{ba}^{cl}(y_m) \}^{-1} \left\{ \frac{d\sigma_{ab}}{dy_2 dt_2} \right\} \quad (39)$$

where  $\sigma_{ba}^{cl}(y_m) = \beta_b \beta_a e^{\epsilon y_m}$ . This **clean** prediction involves no new parameter, with the understanding that, when  $y_m$  is low, secondary terms must be added.

## 7.2 Prediction for DD Cross Sections:

For double diffraction dissociation (DD), there are two large missing mass variables,  $M_1^2$ ,  $M_2^2$ , separated by one large rapidity gap,  $y$ , and its associate momentum transfer variable  $t$ . Again, for  $t$  small, we have the constraint  $y_{m_1} + y_{m_2} + y \simeq Y$ .

The classical differential DD cross section is  $\sigma_{a,\mathcal{P}}^{cl}(y_{m_1}) \bar{F}_{\mathcal{P}}^{cl}(y, t) \sigma_{b,\mathcal{P}}^{cl}(y_{m_2})$ , where the classical “gap distribution” function is  $\bar{F}_{\mathcal{P}}^{cl}(t, y) = (1/16\pi) e^{2(\epsilon + \alpha'_{\mathcal{P}} t)y}$ . After taking care of both flavoring and final-state screening, one obtains for the renormalization factor

$$Z_{DD}(y_{m_1}, y, t, y_{m_2}) = R(M_1^2) [\bar{S}_f(y, t) R(y)^2] R(M^2) \equiv Z_m(M_1^2) \bar{Z}_d(\xi, t) Z_m(M_2^2). \quad (40)$$

A new screening factor,  $\bar{S}_f(y, t)$ , has to be introduced because of the difference in the  $t$ -distribution associated with two factors of triple-Pomeron coupling. It can be obtained from  $S_f(y, t)$  by replacing  $B_d(y)$  by  $\bar{B}(y) = \bar{b} + \alpha'_{\mathcal{P}} t$ , where, by factorization,  $\bar{b} = 2b_d - b_0$ , ( $\bar{b}$  is the  $t$ -slope associated with the triple-Pomeron coupling).

Alternatively, this cross section can again be expressed as a product of two single diffractive cross sections

$$\frac{d\sigma_{ab}}{dy_{m_1} dt dy_{m_2}} = \left\{ \frac{d\sigma_{ab}}{dy_{m_1} dt} \right\} \{ \bar{Z}_d(y, t) \sigma_{ab}^{el}(y, t) \}^{-1} \left\{ \frac{d\sigma_{ab}}{dy_{m_2} dt} \right\}, \quad (41)$$

where  $\sigma_{ab}^{el}(y, t) \equiv (1/16\pi) |\beta_a(t) \beta_b(t) e^{(\epsilon + \alpha'_{\mathcal{P}} t)y}|^2$ . Other than the modification from  $S_f$  to  $\bar{S}_f$ , this prediction is again given uniquely in terms of the single diffraction dissociation cross sections.

### 7.3 Other Gap Cross Sections

We are now in the position to write down the general Pomeron contribution to the differential cross section with an arbitrary number of large rapidity gaps. For instance, generalizing the DPE process to an  $n$ -Pomeron exchange process, there will now be  $n$  large rapidity gaps, with  $n - 1$  short-range ordered missing mass distributions alternating between two gaps. The corresponding renormalization factor is

$$Z_{PE}^{(n)} = Z_d(\xi_1, t_1) Z_m(M_1^2) \bar{Z}_d(\xi_2, t_2) Z_m(M_2^2) \cdots Z_m(M_{n-1}^2) Z_d(\xi_n, t_n). \quad (42)$$

Other generalizations are all straight forward. However, since these will unlikely be meaningful phenomenologically in the near future, we shall not discuss them here. It is nevertheless interesting to point out that, if any cross section does become meaningful experimentally, flavoring would dictate that it is most likely the classical triple-Regge formulas with  $\alpha_{\mathcal{P}}(0) \simeq 1$  that would be at work first.

## 8 Comments:

Let us briefly recapitulate what we have accomplished. Given Pomeron as a pole, the total Pomeron contribution to a singly diffractive dissociation cross section can in principle be expressed as

$$\frac{d\sigma}{dt d\xi} = [S_i(s, t)] [F_{a,\mathcal{P}}(\xi, t)] [\sigma_{\mathcal{P}b}(M^2)], \quad (43)$$

$$F_{a,\mathcal{P}}(\xi, t) = S_f(\xi, t) F_{\mathcal{P}/a}(\xi, t) \quad (44)$$

- The first term,  $S_i$ , represents initial-state screening correction. We have demonstrated that, with a Pomeron intercept greater than unity and with a pole approximation for total and elastic cross sections remaining valid, initial-state absorption cannot be large. We therefore can justify setting  $S_i \simeq 1$  at Tevatron energies.
- The first crucial step in our alternative resolution to the Dino's paradox lies in properly treating the final-state screening,  $S_f(\xi, t)$ . We have explained in an expanding disk setting why a final-state screening can set in relatively early when compared with that for elastic and total cross sections.

- We have stressed that the dynamics of a soft Pomeron in a non-perturbative QCD scheme requires taking into account the effect of “flavoring”, the notion that the effective degrees of freedom for Pomeron is suppressed at low energies. As a consequence, we find that  $F_{\mathcal{P}/a}(\xi, t) = R^2(\xi^{-1})F_{\mathcal{P}/a}^{cl}(\xi, t)$  and  $\sigma_{\mathcal{P}b}(M^2) = R(M^2)\sigma_{\mathcal{P}b}^{cl}(M^2)$  where  $R$  is a “flavoring” factor.

It is perhaps worth contrasting what we have achieved with the flux renormalization scheme of Goulianos. [5] By construction, the normalization factor  $N(s)$  is of the form which one would have obtained from an initial-state screening consideration. Although this breaks factorization, one might hope perhaps the scheme could be phenomenologically meaningful at Tevatron energies. Note that, for  $\sqrt{s} > 22 \text{ GeV}$ , the renormalization factor  $N(s)$  has an approximately factorizable form:  $N(s) \sim .25 s^{2\epsilon} = .25 (\xi^{-1})^{2\epsilon} (M^2)^{2\epsilon}$ . it follows that the diffractive differential cross section remains in a factorized form:

$$\xi \frac{d\sigma^{sd}}{dtd\xi} \sim .25 [\xi^{2\epsilon+1} F_{\mathcal{P}/p}^{(0)}(\xi, t)] [(M^2)^{-2\epsilon} \sigma_{\mathcal{P}p}^{(0)}(M^2, t)]. \quad (45)$$

It can be shown that Eq. (45) leads to a diffractive cross section  $\sigma^{sd}$  which, up to  $\log s$ , is asymptotically constant. That is, the diffractive dissociation contribution no longer corresponds to the part of total cross sections represented by the Pomeron exchange. This is not in accord with the basic hypothesis of Pomeron dominance for total and elastic cross sections at Tevatron energies. [24]

Our final resolution shares certain common features with that proposed by Schlein. [8] At a fixed  $\xi$ ,  $Z_m(M^2) \simeq 1$  as  $s \rightarrow \infty$  so that it is possible to identify our renormalization factor  $Z_d(\xi, t) = S_f(\xi, t)R^2(\xi^{-1})$  with the flux damping factor  $Z_S(\xi)$  of Schlein. In Ref. [8], it was emphasized that the behavior of  $Z_S(\xi)$  can be separated into three regions. (i)  $(\xi_1, \xi_{max})$  where  $Z_S \simeq 1$ , (ii)  $(\xi_2, \xi_1)$  where  $Z_S$  drops from 1 to 0.4 smoothly, and (iii)  $(0, \xi_2)$  where  $Z_S(\xi) \rightarrow 0$  rapidly as  $\xi \rightarrow 0$ . The boundaries of these regions are  $\xi_1 \sim 0.015$  and  $\xi_2 \sim 10^{-4}$ . The first boundary  $\xi_1$  can be identified with our energy scale,  $s_r \sim \xi_1^{-1} \sim e^{y_r}$ . If we identify the boundary between region-(ii) and region-(iii) with our flavoring scale  $y_f$  by  $s_f^{-1} = e^{-y_f} = \xi_2$ , one has  $y_f \simeq 9$ , which is consistent with our estimate. Since  $S_f(\xi, t) \simeq 1$  for  $\xi > s_f^{-1}$  and  $R^2(\xi^{-1})$  drops from  $R^2(1) \simeq s_f^{2\epsilon}$  to 1 at  $s_f$ , their  $Z_S(\xi)$  behaves qualitatively like our renormalization factor. If one indeed makes this connection, what had originally been a mystery for the origin of the scale,  $\xi_2$ , can now be related to the non-perturbative dynamics of Pomeron

flavoring. [25]

It should be stressed that our discussion depends crucially on the notion of soft Pomeron being a factorizable Regge pole. This notion has always been controversial. Introduced more than thirty years ago, Pomeron was identified as the leading Regge trajectory with quantum numbers of the vacuum with  $\alpha(0) \simeq 1$  in order to account for the near constancy of the low energy hadronic total cross sections. However, as a Regge trajectory, it was unlike others which can be identified by the particles they interpolate. With the advent of QCD, the situation has improved, at least conceptually. Through large- $N_c$  analyses and through other non-perturbative studies, it is natural to expect Regge trajectories in QCD as manifestations of “string-like” excitations for bound states and resonances of quarks and gluons due to their long-range confining forces. Whereas ordinary meson trajectories can be thought of as “open strings” interpolating  $q\bar{q}$  bound states, Pomeron corresponds to a “closed string” configuration associated with glueballs. However, the difficulty of identification, presumably due to strong mixing with multi-quark states, has not helped the situation in practice. In a simplified one-dimensional multiperipheral realization of large- $N$  QCD, the non-Abelian gauge nature nevertheless managed to re-emerge through its topological structure. [16]

The observation of “pole dominance” at collider energies has hastened the need to examine more closely various assumptions made for Regge hypothesis from a more fundamental viewpoint. It is our hope that by examining Dino’s paradox carefully and by finding an alternative resolution to the problem without deviating drastically from accepted guiding principles for hadron dynamics, Pomeron can continued to be understood as a Regge pole in a non-perturbative QCD setting. The resolution for this paradox could therefore lead to a re-examination of other interesting questions from a firmer theoretical basis. For instance, to be able to relate quantities such as the Pomeron intercept to non-perturbative physics of color confinement represents a theoretical challenge of great importance.

## Acknowledgments:

I would like to thank K. Goulianos for first getting me interested in this problem during the Aspen Workshop on Non-perturbative QCD, June 1996. Intensive discussions with K. Goulianos, A. Capella, and A. Kaidalov at Rencontres de Moriond, March, 1997, have been extremely helpful. I am

also grateful to P. Schlein for explaining to me details of their work and for his advice. I want to thank both K. Goulianos and P. Schlein for helping me to understand what I should or should not believe in various facets of diffractive data! Lastly, I really appreciate the help from K. Orginos for both numerical analysis and the preparation for the figures. This work is supported in part by the D.O.E. Grant #DE-FG02-91ER400688, Task A.

## References

- [1] This review is written in honor of Richard Slansky, who helped me greatly in appreciating the importance of understanding inelastic production as the origin of diffractive processes. In this article, which replaces an earlier draft (hep-ph/9706276), we concentrate on soft diffractive production. In a future article, we plan to discuss the relation between soft and hard Pomeron, [3] with particular emphasis on the “flavoring” mechanism leading to the picture of a “Heterotic Pomeron”, (hep-ph/9302308).
- [2] For fits for soft Pomeron parameters, see: A. Donnachie and P. V. Landshoff, Phys. Lett. **B** 296 (1992) 227; J. R. Cudde, K. Kang, and S. K. Kim, Phys. Lett., **B** 395 (1997) 311; R. J. M. Covolan, J. Montanha, and K. Goulianos, Phys. Lett., **B** 389 (1996) 176; M. Block, to be presented at VIIth Blois Workshop on Elastic and Diffractive Scattering, Seoul, June 10-14, 1997.
- [3] G. Ingelman and P. Schlein, Phys. Lett. **B** 296 (1992) 227.
- [4] We use  $s_0 = 1 \text{ GeV}^2$  as the basic energy scale throughout this paper. These “classical” expressions are:  $F_{\mathcal{P}/a}^{cl}(\xi, t) = (1/16\pi)\beta_a(t)^2(\xi^{-1})^{2\alpha_{\mathcal{P}}(t)-1}$ , and  $\sigma_{\mathcal{P}b}^{cl}(M^2, t) = g(t)(M^2)^{\alpha_{\mathcal{P}}(0)-1}\beta_b(0)$ . The triple-Pomeron coupling  $g(t)$  can be in principle determined by data below  $\sqrt{s} \leq 30 \text{ GeV}$  where cross sections are relatively insensitive to the choice of the Pomeron intercept value used. As far as I am aware of, the first attempt in using a “triple-Regge” analysis to interpret real experimental data was made by: D. Silverman and C-I Tan, “Relation Between the Multi-Regge Model and the Missing-Mass Spectrum”, Phys. Rev., **D2** (1970) 233. A formal postulation was first made by DeTar, Jones, Low, Tan, Weis, and Young, Phys. Rev. Letters, **26** (1971) 675. For other contemporaneous works, see: D. Horn



and F. Zachariasen, “Hadron Physics at Very High Energies”, (Benjamin, 1973).

- [5] K. Goulianos, Phys. Lett., **B** 358 (1995) 379.
- [6] This “renormalization” factor is chosen so that the new “Pomeron flux”,  $F_N(s, \xi, t) \equiv N(s)^{-1} F_{\mathcal{P}/p}^{cl}(\xi, t)$ , is normalized to unity for  $s \geq \bar{s}$ ,  $\sqrt{\bar{s}} \simeq 22 \text{ GeV}$ . With  $\xi_{min}(s) = 1.5/s$ ,  $\xi_{max} = 0.1$ ,  $\epsilon \simeq .08$ ,  $N(s) \equiv \int_{-\infty}^0 dt \int_{\xi_{min}}^{\xi_{max}} F_{\mathcal{P}/p}^{cl}(\xi, t) d\xi \simeq .25 s^{2\epsilon} > 1$ , for  $\sqrt{s} \geq 22 \text{ GeV}$ , and  $N(s) \equiv 1$  for  $\sqrt{s} \leq 22 \text{ GeV}$ .
- [7] K. Goulianos, Proceedings of the 3rd Workshop on Small-x and Diffractive Physics, Argonne National Laboratory, USA, September 1996; K. Goulianos, Proceedings of the 5th International Workshop on Deep Inelastic Scattering and QCD (DIS-97), Chicago, USA, April 1997.
- [8] P. Schlein, Proceedings of the 3rd Workshop on Small-x and Diffractive Physics, Argonne National Laboratory, USA, September 1996; P. Schlein, Proceedings of the 5th International Workshop on Deep Inelastic Scattering and QCD (DIS-97), Chicago, USA, April 1997.
- [9] S. Erhan and P. Schlein, “Saturation of the Pomeron Flux Factor in the Proton by Damping Small Pomeron Momenta”, to be submitted to Phys. Lett. For a difference in opinion, see Ref. [10]. See also: A. Brandt, et al., “Measurements of Single Diffraction at  $\sqrt{s} = 630 \text{ GeV}$ ; Implication for the Pomeron Flux Factor”, to be submitted to Nucl. Phys.
- [10] K. Goulianos, “Comments on the Erhan-Schlein Model of Damping the Pomeron Flux at Small-x”, hep-ph/9704454.
- [11] E. Gotsman, E. M. Levin, and U. Maor, Phys. Rev., **D49** (1994) 4321.
- [12] T. K. Gaisser and C-I Tan, Phys. Rev., **D8** (1973) 3881; C-I Tan, Proc. IX Rencontres de Moriond, Meribel, France (1974). We include both  $N\bar{N}$  and  $c\bar{c}$  production as well as other effects. The effective degrees of freedom involved are “diquarks” and charm quarks respectively. For color counting, a baryon is considered as a bound state of a quark and diquark. In a more modern approach, baryons are to be considered as skyrmions in a large  $N$  approach. Again, they should be treated as independent degrees of freedom from mesons. See also: J. W. Dash and S. T. Jones, Phys. Lett., **B** 157 (1985) 229.

- [13] C-I Tan, Proc. of 2nd International Conference on Elastic and Diffractive Scattering, ed. K. Goulianos, (Editions Frantieres, 1987) p347; C-I Tan, Proc. of XIXth International Symposium on Multiparticle Dynamics, Arles, ed. D Schiff and J. Tran T. V. (Editions Frontieres, 1988) p361. We do not include “semi-hard” production in the current treatment for soft Pomeron. Flavoring will indeed be the primary mechanism in our construction of a “Heterotic Pomeron”.
- [14] H. Harari, Phys. Rev. Lett. **20** (1968) 1395; P. G. O. Freund, Phys. Rev. Lett. **20**, 235 (1968).
- [15] W. Frazer, D. R. Snider and C-I Tan, Phys. Rev., **D8** (1973) 3180.
- [16] H. Lee, Phys. Rev. Lett., **30** (1973) 719; G. Veneziano, Phys. Lett., **B** 43 (1973) 314. See also, F. Low, Phys. Rev. **D** 12 (1975) 163. A phenomenological realization of QCD emphasizing the topological structure of large-N gauge theories is Dual Parton Model, (DPM). For a recent review, see: A. Capella, U. Sukhatme, C-I Tan, and J. Tran T. V., Physics Reports, **236** (1994) 225.
- [17] For diffraction dissociation,  $c$  must have same quantum numbers as the incident particle  $a$ . For definiteness, we discuss leading particle gap distribution relative to the incoming particle  $a$  with a positive, large rapidity, and assume  $c = a$ . For  $p\bar{p}$  collision, actual diffractive cross section,  $\sigma^{sd}$ , is arrived at by taking into account contributions involving diffraction at both  $p$  and  $\bar{p}$  vertices.
- [18] This mechanism has been recognized before. It was used in Ref. [19] to explain why a “maximal odderon” cannot be allowed in any hadronic scheme which admits an expanding-disk interpretation at high energies.
- [19] G. Finkelstein, H. M. Fried, K. Kang, and C-I Tan, Phys. Lett., **B** 232 (1989) 257.
- [20] It is possible also to apply an eikonal model to study initial state screen for singly diffractive dissociation cross section. This indeed has been performed before, however, without taking final-state screening into account. [11] The fact that inelastic absorption takes place at small impact parameter, with surviving scattering allowed only at the edge of the expanding disk has also been noted there. Since our final-state absorption would remove all scattering within the disk, applying an eikonal initial-state absorption procedure becomes unnecessary.

- [21] By choosing  $\epsilon^{old} < 0$ , it is possible to provide a global “average” description mimicking “secondary trajectory” contributions for various low energy regions. In Ref. [12], acceptable estimates are  $\epsilon_o \simeq -0.11 \sim -0.5$ .
- [22] R. L. Cool, K. Goulianos, S. L. Segler, H. Sticker and S. N. White, Phys. Rev. Lett. **47** (1981) 701.
- [23] The published CDF  $\sigma^{sd}$  values at  $\sqrt{s} = 546$  and  $1800 \text{ GeV}$  are  $7.89 \pm 0.33 \text{ mb}$  and  $9.46 \pm 0.44 \text{ mb}$  respectively. These values correspond to  $\xi_{max} = 0.15$ . We shall restrict  $\xi < 0.05$  and  $t$  to be inside the extreme forward peak. For  $\xi_{max} = 0.05$ , we reduce these values by  $\sim 8\%$  while maintaining their relative ratio of 0.834. For  $t$  to be within the extreme forward diffraction peak we scale down the ISR diffractive cross sections also by approximately 8%. This is appropriate for our determination of the triple-Pomeron coupling.
- [24] Ultimately, these two schemes can be differentiated by confronting experimental data. For our scheme, because of Pomeron pole dominance, it leads to a normalizable limiting gap distribution,  $\rho_a(y; Y)$ , *i.e.*,  $\rho(y, t; Y) \rightarrow \rho_a(y, t)$ . For  $y < y_f \ll Y$ , it is cut-off in  $y$  at least as fast as  $\rho_a(y, t) \propto e^{-\epsilon y}$ . In contrast, the flux renormalization scheme, Eq. (45), leads to a gap distribution of the form  $\rho_a(y; Y) \propto e^{-2\epsilon Y} e^{\epsilon y}$ , for  $1 \ll y \ll Y$ . Test of these two alternatives for either the normalization and the  $y$ -distribution can in principle be carried out by comparing data at two Tevatron energies by focusing on the region of fixed small  $t$  and  $0.02 \geq \xi \geq 0.002$ , ( $y_{min} < y < y_f$ ). Interestingly, both behaviors seem to provide acceptable fits based on data presented in Ref. [10].
- [25] There are also several differences between our result and that of Schlein. First, our renormalization factor  $Z(\xi, t; s)$  is  $t$ -dependent whereas Schlein’s is not. At very small  $\xi$ , our suppression factor does not vanish as fast as that of Schlein: ( $Z_S(\xi) \sim \xi$ , whereas ours behaves as  $\xi^{2\epsilon}$ ). Furthermore, since we have found that there is very little screening needed at Tevatron energies, our slow cutoff might not set in until much higher energies so that it could indeed be possible to observe the  $\xi^{-2\epsilon}$  behavior for  $d\sigma^{sd}/dydt$  at Tevatron energies.